ARTICLE IN PRESS

Manufacturing Letters xxx (xxxx) xxx

Contents lists available at ScienceDirect

Manufacturing Letters

journal homepage: www.elsevier.com/locate/mfglet

Aerosol printing and flash sintering of conformal conductors on 3D nonplanar surfaces

I-Meng Chen [a,1], Yangtao Liu [b,1], Xiaowei Yu [a,*,1], Wesley Everhart [c], Jonghyun Park [a], Yan Wang [b,*], Heng Pan [a,d,*]

[a] Department of Mechanical and Aerospace Engineering, Missouri University of Science and Technology, Rolla, MO 65401, United States
[b] Department of Mechanical Engineering, Worcester Polytechnic Institute, Worcester, MA 01609, United States
[c] Honeywell Federal Manufacturing & Technologies LLC, Kansas City National Security Campus, Kansas City, MO 64147, United States
[d] J. Mike Walker's 66 Department of Mechanical Engineering, Texas A&M University, College Station, TX 77843, United States

ARTICLE INFO

Article history:
Received 25 January 2021
Received in revised form 21 August 2021
Accepted 7 September 2021
Available online xxxx

Keywords:
Conformal conductors
Copper nanoparticles
Aerosol printing
Flash sintering
Printed electronics

ABSTRACT

Printing techniques have been extensively studied as a promising route towards large-scale, low-cost and high-throughput manufacturing process for electronic devices. With the recently emerging applications in wearable electronics and customizable conformal electronics, it calls for the necessity to develop printed electronics that function on complex, 3D nonplanar architectures. In this study, aerosol printing and flash sintering of conformal conductors on nonplanar surfaces are demonstrated. Various printed patterns are fabricated by aerosol printing of conductive ink by copper nanoparticles (Cu NPs) on both planar and nonplanar surfaces. Pulsed flash light introduces rapid sintering of the printed Cu patterns in the ambient environment. For the nonplanar patterns, a back reflector is utilized to improve the uniformity of sintering. As a result, highly conductive customizable nonplanar Cu patterns with conductivity at 10%–12% of that of bulk Cu are obtained. Effects of different sintering conditions, including sintering voltage and mounting distance on the conductivity of sintered patterns are studied. For nonplanar patterns, conductivity values at different localized spots on the nonplanar rod are also investigated to evaluate the uniformity of nonplanar sintering. The processes of aerosol printing and flash sintering have provided a facile manufacturing route for conformal conductors on arbitrary nonplanar objects.

1. Introduction

Printing techniques have been extensively developed as a promising route towards large-scale, low-cost and high-throughput manufacturing process [1–4] for various electronic devices including radio frequency identification (RFID) tags [5,6], sensors [7,8], transistors [9,10], energy devices [11–14] and memory devices [15,16]. Currently, the devices are mostly printed on 2D planar substrates. For novel applications such as wearable electronics and customizable conformal electronics, it appeals to develop printed electronics that function on complex, 3D nonplanar architectures. 3D nonplanar electronics have been reported by fabrication methods such as conformal transfer printing [17,18] and forming [19,20]. However, these methods require complicated fabrication processes which post difficulty in cost-effective and large-scale manufacturing. Comparatively, direct printing on 3D nonplanar surfaces provides facile process with better flexibility in the fabrication of freeform patterns and architectures [21]. There have been several works demonstrating the printing on 3D nonplanar surfaces with ink containing silver nanoparticles (Ag NPs) [22,23]. Direct printing of Ag inks have also been developed to fabricate free-standing 3D architectures [24,25]. The printing techniques used in these works include extrusion printing [21], inkjet printing [24], and aerosol printing [25]. Among them, aerosol printing has its unique advantage due to the flexible stand-off distance of 1–5 mm from the deposition nozzle to the substrate [26,27], which enables its capability of deposition on substrates with complex surface topologies such as trenches and wavy structures (tens of micron to millimeter size) [28,29]. The nonplanar printing capability can be further extended to large objects (centimeter size) with 5-axis stage equipped [29].

Recently, copper nanoparticles (Cu NPs) have been developed for conductive inks of printed electronics due to the considerably

* Corresponding authors at: Department of Mechanical and Aerospace Engineering, Missouri University of Science and Technology, Rolla, MO 65401, United States (H. Pan).

E-mail addresses: xy5w8@mst.edu (X. Yu), yanwang@wpi.edu (Y. Wang), hp5c7@mst.edu (H. Pan).

[1] These authors contributed equally to this work.

https://doi.org/10.1016/j.mfglet.2021.09.007
2213-8463/

Please cite this article as: I-Meng Chen, Y. Liu, X. Yu et al., Aerosol printing and flash sintering of conformal conductors on 3D nonplanar surfaces, Manufacturing Letters, https://doi.org/10.1016/j.mfglet.2021.09.007

lower cost than the more commonly used Ag NPs [30–32]. In this study, we aimed to fabricate conformal conductors on nonplanar surfaces with Cu NPs. One of the major concerns in the printing of Cu is that Cu is easier to get oxidized compared to Ag. Thermal sintering of Cu usually requires vacuum or inert gas environment to avoid the oxidation issue [33]. Alternatively, sintering techniques employing high energy irradiation have been recently reported to sinter Cu NPs in ambient environment [34–36]. Among these methods, flash sintering relies on the wide wavelength spectrum of the emitted light to heat up the deposited materials over a relatively large projected area [34,37]. It is used in this study to accommodate the 3D complex geometries of the printed patterns with a back reflector introduced to improve the uniformity of sintering.

2. Manufacturing methods

Aerosol printing and flash sintering are used for the printing and sintering of highly conductive Cu patterns. Both methods are developed with nonplanar processing capabilities to realize printing and sintering on 3D nonplanar surfaces. This section provides a brief introduction to these two manufacturing methods. Experimental details are given in Supplementary Material.

2.1. Nonplanar aerosol printing

Schematic of the nonplanar aerosol printing system is shown in Fig. 1a. The system consists of nebulizer, deposition nozzle, sample mount and 5-axis stage. In the nebulizer, aerosol mists containing microparticles of the solvent and Cu NPs are generated and delivered to the deposition nozzle by the carrier gas. The substrate for printing is Kapton® polyimide (PI). The 5-axis stage provides translational motion in three directions and rotational motion in two directions to realize printing on nonplanar surfaces.

2.2. Nonplanar flash sintering

Schematic of the nonplanar flash sintering system is shown in Fig. 1b. Pulsed flash light from a Xenon lamp is capable of rapid sintering of the printed patterns in ambient environment with a pulse duration of 2 ms. A back reflector with adjustable height and angle is mounted to realize nonplanar flash sintering with improved uniformity of sintering. Fig. 1c displays different nonplanar patterns on cylindrical substrates in spiral and square wave. Fig. 1d gives a demonstration on the printed and sintered conformal Cu conductor on a piece of earring as the nonplanar mounting object. Fig. 1e presents the photograph of the conformal Cu conductor on a rod substrate during the nonplanar flash sintering process.

3. Results and discussion

The aerosol printed Cu patterns before and after sintering are shown in Fig. 2a-b. After flash sintering, the Cu patterns remained intact. The color of the Cu patterns turned from black to metallic light orange, indicating the formation of conductive Cu. To understand the transformation of microstructures of the printed Cu patterns before and after flash sintering, they were examined by scanning electron microscopy (SEM). Before flash sintering (Fig. 2c), the unsintered Cu NPs were mostly individually segregated. After flash sintering (Fig. 2d), the growth in the particle diameter of Cu NPs was observed (Fig. S1). The Cu NPs showed fused contact with the neighboring particles, which was essential to the formation of conductive path.

The oxidation on the surface of the flash sintered Cu patterns were evaluated by energy dispersive spectroscopy (EDS) and compared to the unsintered Cu patterns. The EDS spectra for the flash sintered and unsintered Cu patterns were shown in Fig. S2a-b. It was found that the wt% of oxygen was reduced after flash sintering, which indicated the sintering in ambient condition did not introduce oxidation of the Cu NPs. Instead, the reduced wt% of oxygen

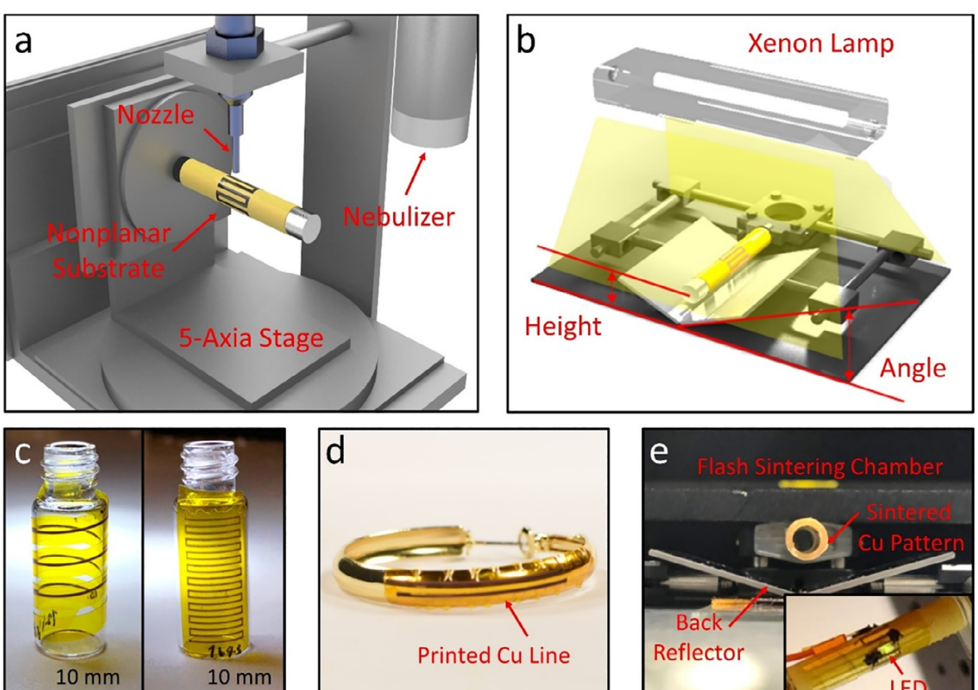

Fig. 1. Schematics of (a) nonplanar aerosol printing and (b) nonplanar flash sintering of conformal Cu conductors. (c) Photograph of the nonplanar Cu patterns in spiral and square wave. (d) Photograph of the conformal Cu conductor on nonplanar object (earring) as a demonstration. (e) Photograph of the conformal Cu conductor on a rod substrate during the nonplanar flash sintering process. Inset photograph shows the conformal conductor as the interconnect for the LED circuit.

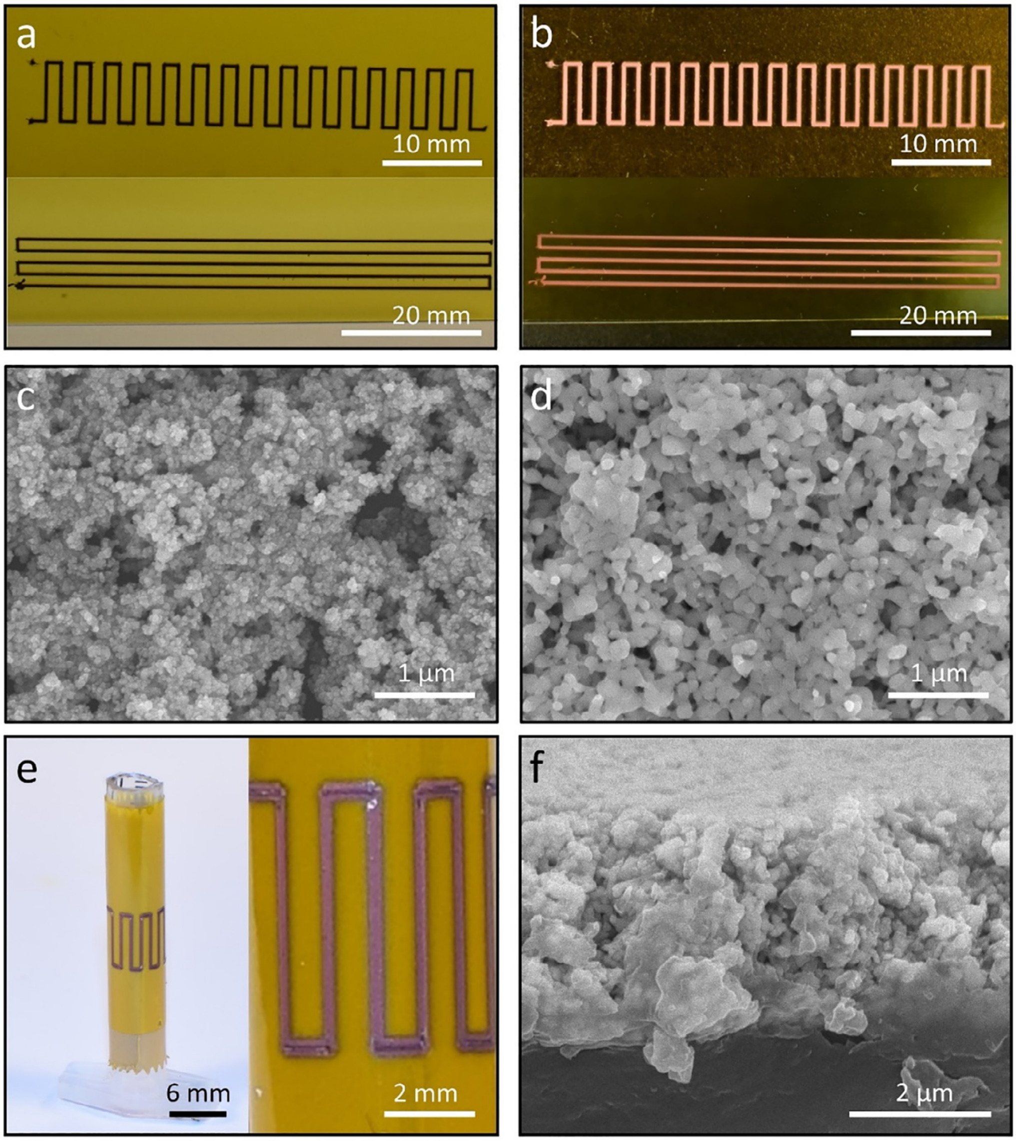

Fig. 2. (a) Photographs of the sintered and (b) unsintered Cu patterns. (c) SEM images of the printed Cu NPs before sintering and (d) after sintering. (e) Optical microscopic images of the nonplanar Cu patterns. (f) cross-section SEM image the nonplanar Cu patterns.

could reveal the reduction of readily formed oxides on the surface of Cu patterns, as the flash sintering of CuO nanoparticles into Cu conductive patterns was reported [34]. Another testing was carried out by the thermal sintering of printed Cu patterns in Argon-filled glove box at 300 °C for 1 h. The EDS spectrum of the thermally sintered Cu patterns was shown in Fig. S3c. The wt% of oxygen did not reduce for the thermally sintered Cu patterns. The results indicated that flash sintering could be advantageous to suppress the formation of oxides in printed Cu patterns.

The printed nonplanar Cu patterns (Fig. 2e) on a cylindrical substrate were also examined. The nonplanar patterns were found to be continuous and have similar linewidth to the planar patterns. From the cross-section SEM image in Fig. 2f, the Cu NPs in the nonplanar patterns were well sintered with the same microstructures observed in the planar sintered patterns. At the interface between PI substrate and the printed Cu structure, the materials were observed to be fused together. The formation of the fused interface could come from the partial melting of the PI by the rapid heat introduced during the flash sintering process. The thickness of the printed and sintered Cu pattern was around 2–3 µm.

Effects of different sintering conditions including sintering voltage and mounting distance on the conductivity of sintered patterns were studied for both planar and nonplanar patterns with 10 samples measured for each condition. It was found that optimized sintering conditions for the nonplanar patterns were different from those of the general planar sintering. As seen in Fig. 3a, the optimized conductivity on planar surfaces (with conductivity of 7.7×10^6 S/m and conductivity ratio of ~13%) was found at sintering voltage of 2.1 kV. However, the best result out of nonplanar surfaces (with conductivity of 7.1×10^6 S/m and conductivity ratio of ~12%) was found at voltage of 2.7 kV. As for the mounting height (Fig. 3b-c), the optimized heights for planar sample and nonplanar sample were 4.5 mm and 10.8 mm respectively. The results indicated that mechanism of nonplanar sintering could be different from the planar sintering due to the geometric factors and should be further studied.

For the next step, the sintering effect at different localized spots on the nonplanar rod was investigated. Generally, for planar patterns, the flash light was normally incident on all locations with same traveling distance. This resulted in a uniform light distribu-

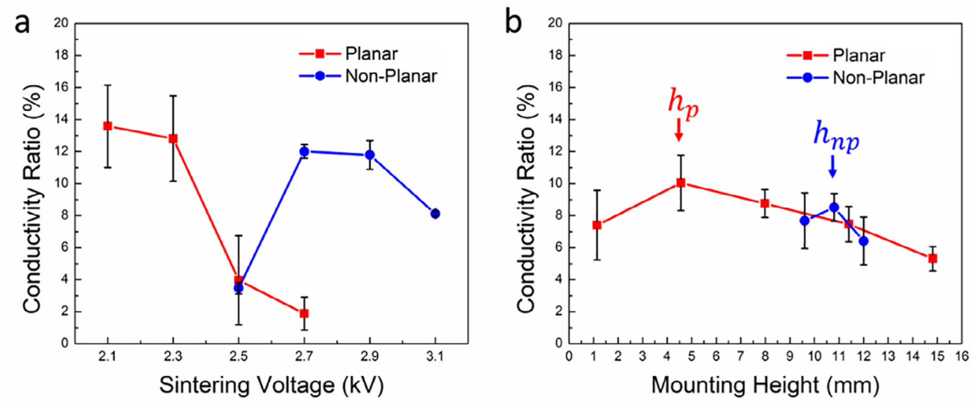

Fig. 3. Conductivity ratios with (a) varied sintering voltage and (b) varied mounting height for planar and nonplanar samples. (c) Schematics explaining mounting height during the sintering process.

tion during the planar sintering. However, without extra designs to help distribute the flash light on different locations on nonplanar surfaces, such configuration would not work for nonplanar sintering. Fig. 4a showed that with 1-time flash sintering, only the half of the rod facing the lamp was sintered, and the conductivity started to degrade from 0° to ±90°. In order to sinter the back side, 2-time flash sintering was introduced by flipping over the rod for 180° and sintering again. However, after the 2-time flash sintering, only the locations near 0° and 180° showed good conductivity while the locations on the side parts of the rod (near ±90°) remained almost unsintered. To improve the sintering uniformity, a back reflector was introduced. The horizontal back reflector (mirror) was initially investigated. However, as shown in Fig. 4b, it did not help enhance the conductivity at any locations because the light was not effectively reflected onto the surface. Then, the tilted angle of the back reflector, which altered the direction of the reflected light was introduced. Fig. 4c indicated that the conductivity was significantly increased at ±90° with the additional angled back reflector applied. The conductivity ratio was measured to be averaging 10% on the cylindrical rod, with slight drop of conductivity on the side parts.

The effects of sintering conditions on the localized conductivity were also studied. It was found that the conductivity ratio was significantly escalated with sintering voltage increased from 2.5 kV to 2.7 kV at all the locations on the rod (Fig. 4d). The effect of mount-

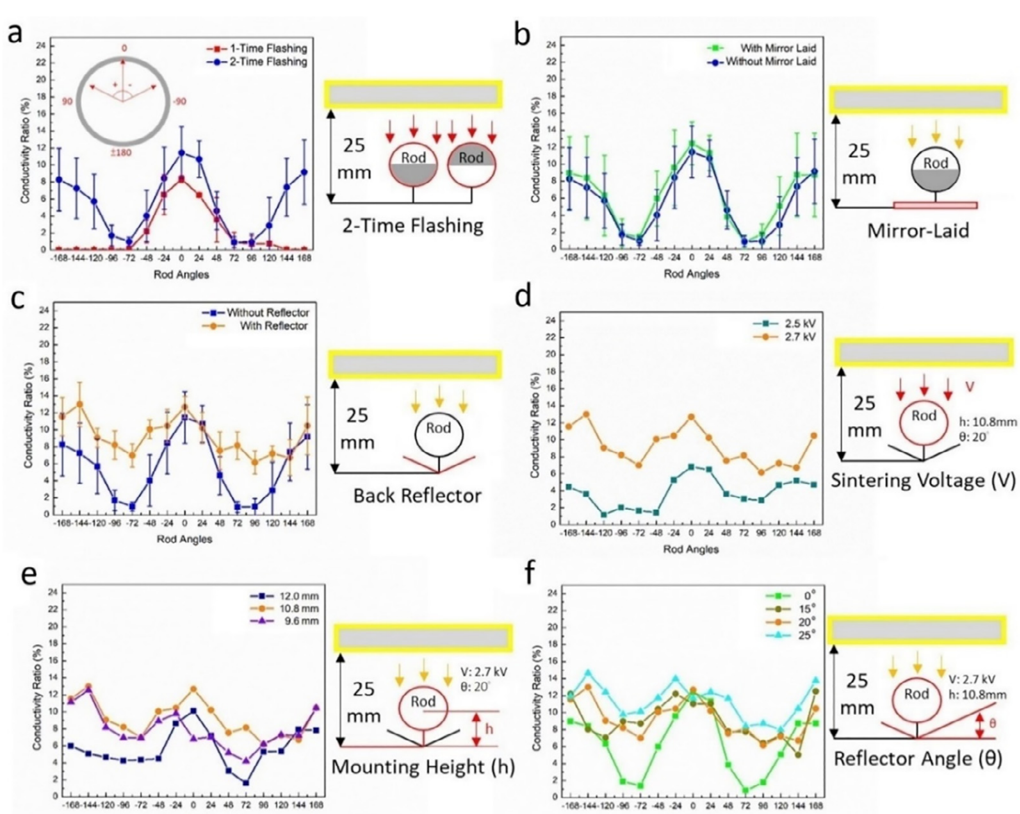

Fig. 4. Conductivity results of localized spots on the nonplanar rod based on (a) flashing times, (b) application of mirror laid, (c) application of back reflector, (d) sintering voltages, (e) mounting heights, and (f) back reflector angles.

ing height was displayed in Fig. 4e. Mounting height of 10.8 mm was observed to provide better sintering results compared to the greater (12.0 mm) or smaller (9.6 mm) heights. In Fig. 4f, effect of different tilted angles of the back reflector on the conductivity ratio at localized spots was presented. It was found that by increasing the angle of back reflector from 0° to 25°, the conductivity ratio was gradually increased and turned to be more uniform. When the back reflector angle was increased to 25°, 80% of the localized spots exhibited conductivity ratio of above 10%. The highest conductivity ratio was ~15% at −144°. Light propagation simulations were performed to calculate the beam density at different localized spots with varied back reflector angles. The results (Fig. S3) showed that the density distribution with back reflector angle at 25° appeared to be the most uniform case, which matched the experiment results.

4. Conclusion

In this study, a new customizable, low-cost, facile manufacturing method of printed conductors on nonplanar surfaces is developed. Aerosol printing is employed to print Cu ink into designed patterns on both planar and nonplanar surfaces with 5-axis stage equipped. Pulsed flash light sinters the printed Cu patterns in the ambient condition. The sintered planar patterns exhibit average conductivity of 7.7×10^6 S/m (~13% of that of bulk Cu). SEM images show the Cu NPs are well coalesced with solid contact to neighboring particles. The nonplanar patterns are well sintered with an angled back reflector at optimized sintering parameters. The conductivity of the nonplanar patterns is found to be 10%–12% of that of bulk Cu. The processes of aerosol printing and flash sintering have provided a facile manufacturing route for conformal conductors on arbitrary nonplanar objects.

Declaration of Competing Interest

The authors declare that they have no known competing financial interests or personal relationships that could have appeared to influence the work reported in this paper.

Acknowledgements

All data prepared, analyzed, and presented has been developed in a specific context of work and was prepared for internal evaluation and use pursuant to that work authorized under the referenced contract. Reference herein to any specific commercial product, process or service by trade name, trademark, manufacturer, or otherwise, does not necessarily constitute or imply its endorsement, recommendation, or favoring by the United States Government, any agency thereof or Honeywell Federal Manufacturing & Technologies, LLC. This paper has been authored by Honeywell Federal Manufacturing & Technologies under Contract No. DE-NA0002839 with the U.S. Department of Energy. The United States Government retains and the publisher, by accepting the article for publication, acknowledges that the United States Government retains a nonexclusive, paid up, irrevocable, world-wide license to publish or reproduce the published form of this manuscript, or allow others to do so, for the United States Government purposes. This work is also supported by the National Science Foundation under Grant No. 1635256 and No. 1846673. The financial supports are greatly appreciated.

Appendix A. Supplementary data

Supplementary data to this article can be found online at https://doi.org/10.1016/j.mfglet.2021.09.007.

References

[1] Rim YS, Bae SH, Chen H, De Marco N, Yang Y. Adv Mater 2016;28:4415.
[2] Leenen MAM, Arning V, Thiem H, Steiger J, Anselmann R. Phys Status Solidi A 2009;206:588.
[3] Perelaer J, Smith PJ, Mager D, Soltman D, Volkman SK, Subramanian V, et al. J Mater Chem 2010;20:8446.
[4] Arias AC, MacKenzie JD, McCulloch I, Rivnay J, Salleo A. Chem Rev 2010;110:3.
[5] Zheng Y, He Z, Gao Y, Liu J. Sci Rep 2013;3:1.
[6] Chiolerio A, MacCioni G, Martino P, Cotto M, Pandolfi P, Rivolo P, et al. Microelectron Eng 2011;88:2481.
[7] Belsey KE, Parry AVS, Rumens CV, Ziai MA, Yeates SG, Batchelor JC, et al. J Mater Chem C 2017;5:3167.
[8] Yeo W-H, Kim Y-S, Lee J, Ameen A, Shi L, Li M, et al. Adv Mater 2013;25:2773.
[9] Fukuda K, Takeda Y, Yoshimura Y, Shiwaku R, Tran LT, Sekine T, et al. Nat Commun 2014;5:1.
[10] Härting M, Zhang J, Gamota DR, Britton DT. Appl Phys Lett 2009;94:1.
[11] Lao-Atiman W, Julaphatachote T, Boonmongkolras P, Kheawhom S. J Electrochem Soc 2017;164:859.
[12] Delannoy PE, Riou B, Brousse T, Le Bideau J, Guyomard D, Lestriez B. J Power Sources 2015;287:261.
[13] Habas SE, Platt HAS, Van Hest MFAM, Ginley DS. Chem Rev 2010;110:6571.
[14] Gaikwad AM, Arias AC, Steingart DA. Energy Technol. 2015;3:305.
[15] Lai Y-C, Huang Y-C, Lin T-Y, Wang Y-X, Chang C-Y, Li Y, et al. NPG Asia Mater 2014;6:e87.
[16] Hosseini NR, Lee JS. Adv Funct Mater 2015;25:5586.
[17] Wu H, Tian Y, Luo H, Zhu H, Duan Y, Huang Y. Adv Mater Technol 2020;5:2000093.
[18] Zhang S, Wang B, Jiang J, Wu K, Guo CF, Wu Z, et al. Mater Interfaces 2019;11:7148.
[19] Devaraj H, Malhotra R. J Manuf Sci Eng Trans ASME 2019;141:1.
[20] Devaraj H, Hwang HJ, Malhotra R. J Manuf Process 2020;58:1088.
[21] Lewis JA. Adv Funct Mater 2006;16:2193.
[22] Adams JJ, Duoss EB, Malkowski TF, Motala MJ, Ahn BY, Nuzzo RG, et al. Adv Mater 2011;23:1335.
[23] Jo Y, Kim JY, Jung S, Ahn BY, Lewis JA, Choi Y, et al. Nanoscale 2017;9:14798.
[24] Vaithilingam J, Saleh E, Körner L, Wildman RD, Hague RJM, Leach RK, et al. Mater Des 2018;139:81.
[25] Saleh MS, Hu C, Panat R. Sci Adv 2017;3:e1601986.
[26] Chen G, Gu Y, Tsang H, Hines DR, Das S. Adv Eng Mater 2018;20:1701084.
[27] Wilkinson NJ, Smith MAA, Kay RW, Harris RA. Int J Adv Manuf Technol 2019;105:4599.
[28] Mahajan A, Frisbie CD, Francis LF. ACS Appl Mater Interfaces 2013;5:4856.
[29] Yu X, Liu Y, Pham H, Sarkar S, Ludwig B, Chen IM, et al. Adv Mater Technol 2019;4:1900645.
[30] Wang Y, Li N, Li D, Yu S, Wang C. Mater Lett 2015;140:127.
[31] Kim S, Bito I, Jeong S, Georgiadis A, Tentzeris MM. In: Proc. 2015 IEEE MTT-S Int. Microw. Symp., Phoenix, USA. p. 1–4.
[32] Hokita Y, Kanzaki M, Sugiyama T, Arakawa R, Kawasaki H. ACS Appl Mater Interfaces 2015;7:19382.
[33] Park BK, Kim D, Jeong S, Moon J, Kim JS. Thin Solid Films 2007;515:7706.
[34] Kang H, Sowade E, Baumann RR. ACS Appl Mater Interfaces 2014;6:1682.
[35] Han S, Hong S, Yeo J, Kim D, Kang B, Yang MY, et al. Adv Mater 2015;27:6397.
[36] Norita S, Kumaki D, Kobayashi Y, Sato T, Fukuda K, Tokito S. Org Electron 2015;25:131.
[37] Mahajan BK, Yu X, Shou W, Pan H, Huang X. Small 2017;13:1700065.